Deep-Sea Research I 106 (2015) 17–29

Contents lists available at ScienceDirect

Deep-Sea Research I

journal homepage: www.elsevier.com/locate/dsri

Influence of the Yellow Sea Warm Current on phytoplankton community in the central Yellow Sea

Xin Liu [a,b,c], Kuo-Ping Chiang [b,c], Su-Mei Liu [d], Hao Wei [e], Yuan Zhao [f], Bang-Qin Huang [a,*]

[a] Key Laboratory of Coastal and Wetland Ecosystems, Ministry of Education; State Key Laboratory of Marine Environmental Science, Xiamen University, 361102 Xiamen, Fujian
[b] Institute of Marine Environmental Chemistry and Ecology, National Taiwan Ocean University, 202-24 Keelung, Taiwan
[c] Center of Excellence for Oceans, National Taiwan Ocean University, Keelung 202-24, Taiwan
[d] Key Laboratory of Marine Chemistry Theory and Technology, Ministry of Education, Ocean University of China, 266100 Qingdao, Shandong
[e] College of Marine Science and Engineering, Tianjin University of Science and Technology, 300222 Tianjin
[f] Key Laboratory of Marine Ecology and Environmental Sciences, Institute of Oceanology, Chinese Academy of Sciences, 266071 Qingdao, Shandong

ARTICLE INFO

Article history:
Received 5 May 2015
Received in revised form
18 September 2015
Accepted 22 September 2015
Available online 9 October 2015

Keywords:
Biogeochemical process
Phytoplankton
Community structure
Yellow Sea
Nutrients
Spring bloom

ABSTRACT

In early spring, a hydrological front emerges in the central Yellow Sea, resulting from the intrusion of the high temperature and salinity Yellow Sea Warm Current (YSWC). The present study, applying phytoplankton pigments and flow cytometry measurements in March of 2007 and 2009, focuses on the biogeochemical effects of the YSWC. The nutrients fronts were coincident with the hydrological front, and a positive linear relationship between nitrate and salinity was found in the frontal area. This contrast with the common situation of coastal waters where high salinity values usually correlate with poor nutrients. We suggested nutrient concentrations of the YSWC waters might have been enhanced by mixing with the local nutrient-rich waters when it invaded the Yellow Sea from the north of the Changjiang estuary. In addition, our results indicate that the relative abundance of diatoms ranged from 26% to 90%, showing a higher value in the YSCC than in YSWC waters. Similar distributions were found between diatoms and dinoflagellates, however the cyanobacteria and prasinophytes showed an opposite distribution pattern. Good correlations were found between the pigments and flow cytometry observations on the pico-phytoplankton groups. Prasinophytes might be the major contributor to pico-eukaryotes in the central Yellow Sea as similar distributional patterns and significant correlations between them. It seems that the front separates the YSWC from the coastal water, and different phytoplankton groups are transported in these water masses and follow their movement. These results imply that the YSWC plays important roles in the distribution of nutrients, phytoplankton biomass and also in the community structure of the central Yellow Sea.

1. Introduction

Western boundary currents, such as the Kuroshio, are warm, swift, narrow oceanic currents found in the western side of the subtropical gyres. The branches of western boundary currents into marginal seas are important reasons for the ecosystem dynamics and complexity (Hu et al., 2015). It is clear that the Kuroshio branches are important drivers of the biogeochemical cycles in the East and South China Seas (Yang et al., 2012; Du et al., 2013).

The Yellow Sea is a semi-enclosed marginal sea with depths ranging from 20 to 90 m, bounded by China and Korean Peninsula and influenced by the East Asian Monsoon, the Kuroshio Current and riverine input. In winter and early spring, a hydrological front emerges in the central Yellow Sea where the warm Yellow Sea Warm Current (YSWC) meets the cold water of the Yellow Sea Coastal Current (YSCC) (Chen, 2009; Lie et al., 2009; Lin and Yang, 2011; Lin et al., 2011). The YSWC is an asymmetric upwind flow and will intrude into the central Yellow Sea along the western side of the Yellow Sea trough from winter to early spring (Lin et al., 2011). It originates from the northward Kuroshio branch current (Cheju Warm Current) and the Taiwan Warm Current in the northern part of the East China Sea (Lin et al., 2011). On the coastal side, the cold fresh YSCC is brought into the central Yellow Sea when the southward flowing current is influenced by winter monsoons (the northwestern monsoon) (Chen, 2009). Therefore, the front showing extreme contrasts between the warm saline

* Correspondence to: College of the Environment and Ecology, Xiamen University, Xiamen 361102 Fujian. Fax: +86 592 2187783.
E-mail address: bqhuang@xmu.edu.cn (B.-Q. Huang).

http://dx.doi.org/10.1016/j.dsr.2015.09.008
0967-0637/

YSWC and the cold fresh YSCC is developed from winter to early spring and provides a dynamic environment during this period.

Since the 1980s, several theories have been suggested concerning the origin and generation of the YSWC, mainly based on current measurements, historical hydrographic data and numerical models (Lie et al., 2001; Huang et al., 2005; Lin and Yang, 2011; Lin et al., 2011; Wang et al., 2012). To date, however, little is known concerning biogeochemical behaves of the YSWC (Liu et al., 2015). Chen (2009) reveals that the YSWC originates from the Kuroshio and Taiwan Warm Current and thus it is relatively warmer, saltier, and nutrient-poor. While, recent studies reveal that the nitrate concentrations in the YSWC reach up to 8 μM (Fu et al., 2009; He et al., 2013; Jin et al., 2013). It was suggested that nutrient concentrations in the YSWC have increased since the end of last century (He et al., 2013; Jin et al., 2013). However, the nutrients sources and their contributions are unclear (Liu et al., 2015). Despite high nutrient concentrations, quite low chlorophyll *a* (Chl *a*) concentrations dominated by picosize phytoplankton in the YSWC during winter were noted by the size-fraction Chl *a* results (Fu et al., 2009). Our previous study also reported low Chl *a* concentrations ($<0.6\ \mu g\ L^{-1}$) and abundant prasinophytes in the YSWC area in March (Liu et al., 2015). In the absence of direct evidence from flow cytometry observation on the spatial distributions of prokaryotic and eukaryotic picophytoplankton, the difference on phytoplankton community structure between the YSWC and the YSCC is still unclear.

During early spring the region of algal bloom coincides with that of the YSWC in the central Yellow Sea (Liu et al., 2015). High temperature and rich nutrients in the YSWC are hypothesized to be one of the explanations for the spring bloom and its succession patterns (Jin et al., 2013; Liu et al., 2015). During April 2007 and 2009, comprehensive observations were made in the China GLOBEC-IMBER Program (Tang et al., 2013). A special issue in the journal of Deep-Sea Research II (volume 97, 2013) provided a comprehensive picture of the spring bloom (Tang et al., 2013). Generally, the spring blooms are observed in the central Yellow Sea at the water depths >50 m (Hyun and Kim, 2003; Xuan et al., 2011; Liu et al., 2015). They typically last for about two months from April to May, and are composed of a series of sub-bloom events that show different dominant species compositions (Tang et al., 2013). Hu et al. (2004) demonstrated that the initiation of a spring phytoplankton bloom is critically related to the water column stability based on a 3-dimensional physical–biological coupled model. Further, Zhou et al. (2013) observed that the changes in stability of the hydrographic structure caused by oceanic and meteorological factors like horizontal advection, tides, wind and solar radiation affect the development of spring blooms in the central Yellow Sea. In addition, the trigger of the spring algal bloom is considered to be the imbalances in predator-prey relations rather than a reflection of rapid cell division (Behrenfeld and Boss, 2014). Sun et al. (2013) revealed that the grazing rates are generally lower than the growth rates during the pre-blooming phase in the central Yellow Sea, while the grazing rate reaches a balance with the growth rate during the blooming phase with the average net growth rates of the community being 0.207 and 0.005 d^{-1} at pre-blooming and blooming stations. This implies the net growth of phytoplankton during pre-blooming is the major cause of the bloom (Sun et al., 2013). Based on these results, the factors that influence community structure and growth of phytoplankton during the initial stage of the spring bloom are very important.

Previous studies in the special issue provide detailed evidence of the change in hydrological conditions (Zhou et al., 2013), nutrient concentrations (Jin et al., 2013) and temporal variation of picophytoplankton during the blooms (Zhao et al., 2013), but the total phytoplankton community structure. We analyzed results of hydrography, nutrients, phytoplankton biomass and composition, focusing on the biogeochemical characteristics, especially phytoplankton community of the YSWC and the YSCC during the pre-blooming phase in the central Yellow Sea. In the present study, phytoplankton pigments and flow cytometry measurements were firstly conducted simultaneously for this study area. Moreover, the nutrients sources of the YSWC and the factors controlling biomass and composition of phytoplankton community will be discussed.

2. Materials and methods

Two cruises were carried out on the R/V Beidou during 17–23 March 2007 and 20–30 March 2009 (Fig. 1), around 1–2 weeks before the satellites-derived Chl *a* maximum occurred (Fig. 3d) (Tang et al., 2013). In addition, two time series observations using surface Lagrangian drifters which lasted 102 h (from 3:00 am 4th April to 9:00 am 8th April) and 126 h (from 3:00 am 9th April to 9:00 am 14th April) respectively were carried out in 2009 at two stations (Stns. B23 and B20, Fig. 1). At Stn. B20, water in the euphotic zone was fundamentally driven by the YSCC and thus moved to the southwest, while tidal signal was relatively strong at Stn. B23 (the YSWC) as indicated by its orbit (Zhou et al., 2013). Hydrographic and nutrients data of the present study can be found

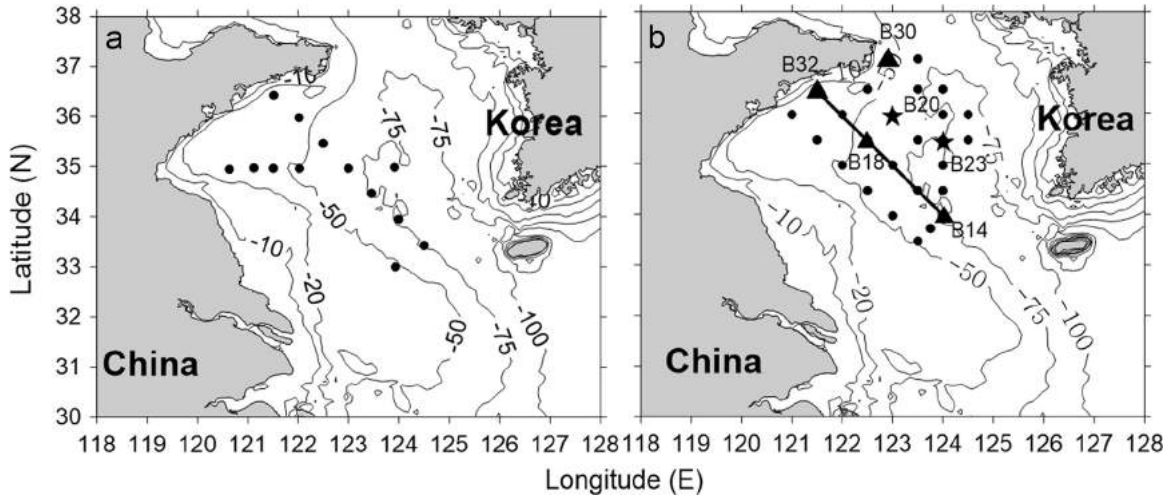

Fig. 1. Map of study area and sampling stations in the Yellow Sea during March 2007 (a) and 2009 (b). The black Triangles and stars indicate the location of Stns. B14, B18, B20, B23, B30 and B32.

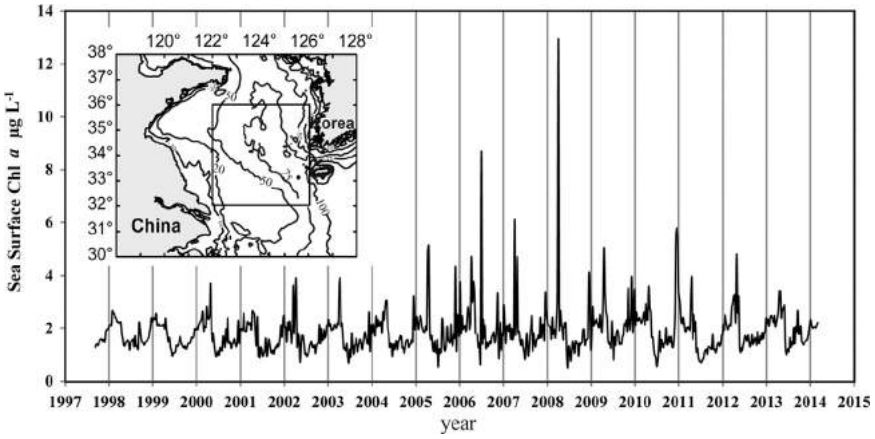

Fig. 2. Long-term variation of sea surface Chl *a* concentration ($\mu g\ L^{-1}$) for a $4^\circ \times 4^\circ$ region (122–126°N by 32–36°E) in the central Yellow Sea.

in Zhou et al. (2013) and Jin et al. (2013), respectively.

Phytoplankton pigments were analyzed using an Agilent series 1100 HPLC system fitted with a 3.5 μm Eclipse XDB C8 column ($4.6 \times 150\ mm^2$, Agilent Technologies, Waldbronn, Germany) (Zapata et al., 2000). Seawater samples for phytoplankton pigment analysis (4–10 L, based on biomass) were filtered through 47 mm GF/F glass fiber filters (under a vacuum pressure less than 75 mm Hg and in dim light), and then were immediately frozen in liquid nitrogen prior to analysis in the laboratory. The following pigments were detected and quantified: Chl *a*, chlorophyll *b*, chlorophyll *c*1+*c*2, chlorophyll *c*3, fucoxanthin (Fuco), 19′-hexanoyloxyfucoxanthin, 19′-butanoyloxyfucoxanthin, prasinoxanthin, lutein, zeaxanthin (Zea), diadinoxanthin, alloxanthin, neoxanthin, violaxanthin and peridinin (Peri). The CHEMTAX program (Mackey et al., 1996) was used to retrieve the group composition of the phytoplankton (diatoms, dinoflagellates, chrysophytes, prymnesiophytes, chlorophytes, cryptophytes, prasinophytes and cyanobacteria). The basis for calculations and the procedures are fully described in Latasa (2007), and the input pigment ratio matrix used in the CHEMTAX calculation was based on a knowledge of the common phytoplankton groups from our previous studies in the Yellow Sea (Liu et al., 2012, 2015).

Flow cytometry samples were fixed with buffered paraformaldehyde (0.5% final concentration) and stored at −80 °C until analysis. Cell abundances of picophytoplankton were enumerated using a FACS Vantage SE flow cytometer (Becton Dickinson) equipped with a water-cooled Argon laser (488 nm, 1 W, Coherent) (Zhao et al., 2013). Protocols were adapted from (Marie et al., 2000) and fluorescent beads (2 μm, Polysciences) were used as the internal standard for the enumeration of picoplankton cells (Olson et al., 1993).

Sea surface temperature (SST) and Chl *a* were extracted from multiple-satellite products (AVHRR, SeaWiFS and MODIS/Aqua). The resolutions of these three databases were 0.044°, 0.1° and 0.05° respectively. A good correlation between the SeaWiFS and MODIS/Aqua data sets was displayed in the Yellow Sea using quantitative comparisons (Liu and Wang, 2013), suggesting that SeaWiFS Chl *a* time series gaps can be directly filled using the corresponding MODIS/Aqua Chl *a* data to enlarge the Chl *a* dataset series (Liu and Wang, 2013). Based on *T*–*S* diagram analysis (Fig. 5) and previous study (Chen, 2009), it is reasonable to separate the coastal water from the YSWC with the salinity <32, and the temperature of these samples were <8 °C. Further, the YSWC and the front area were defined as their salinity >33 and within 32–33, respectively. We performed a canonical correlation analysis (CCA), which is a multidimensional exploratory method that can highlight correlations between two groups of variables (González et al., 2008). A R package was used to perform the regularized extension of CCA (González et al., 2008). A one-way ANOVA was used for statistical analysis following a test the homogeneity of the variances. The significance level was set at $p < 0.05$. ANOVA results were compared using the least significant difference method. The euphotic zone was defined as the upper water column down to the depth at which the downward photosynthetically active radiation was 1% of the value just below the surface. Vertical profiles of light intensity were obtained at each station using a free-fall spectroradiometer (SPMR, Satlantic), just prior to water sampling during the day. This paper mainly describes the results of the cruise in March 2009; similar results were observed in the cruises between 2007 and 2009.

3. Results

3.1. Long-term variation of Chl a and cruise background based on satellite data

Long-term variation of sea surface Chl *a* concentration in a $4^\circ \times 4^\circ$ region (122–126°N by 32–36°E) in the central Yellow Sea displayed a clear seasonal cycle (Fig. 2). The maximum Chl *a* each year occurs in spring (April), but some peaks occasionally appear in summer (e.g. June 2006) or early winter (e.g. December 2010). An increasing trend of spring algal bloom was observed from the end of the last century, but it seems to have declined after 2008 (Fig. 2). Nevertheless, a considerably large interannual variation on Chl *a* is observed.

The monthly mean SST and Chl *a* concentration during March and April 2009 were extracted (Fig. 3). During March, temperatures were higher in the central Yellow Sea (>8 °C) than in the coastal area (<6 °C), associated with the YSWC and the YSCC, respectively. The warm tongue (>8 °C, the YSWC) extended westward as far as 36°N (Fig. 3a). Compared with the distribution of SST in March, the YSWC was weak in April, but a high Chl *a* value ($>8\ \mu g\ L^{-1}$) was observed in the frontal region in April, indicating that a phytoplankton bloom occurred there (Fig. 3d).

3.2. Hydrological setting

Based on field observations, a strong temperature and salinity front was found between the cold, less saline YSCC and the warm, more saline YSWC in the central Yellow Sea (Fig. 4). In addition, the vertical distributions of temperature and salinity show that water column was well mixed in both the YSCC (Stn. B32) and the YSWC (Stn. B14) due to the strong winter monsoon (Fig. 4). However, a two-layer structure in the water column was observed in the narrow frontal area resulting from the high density YSWC

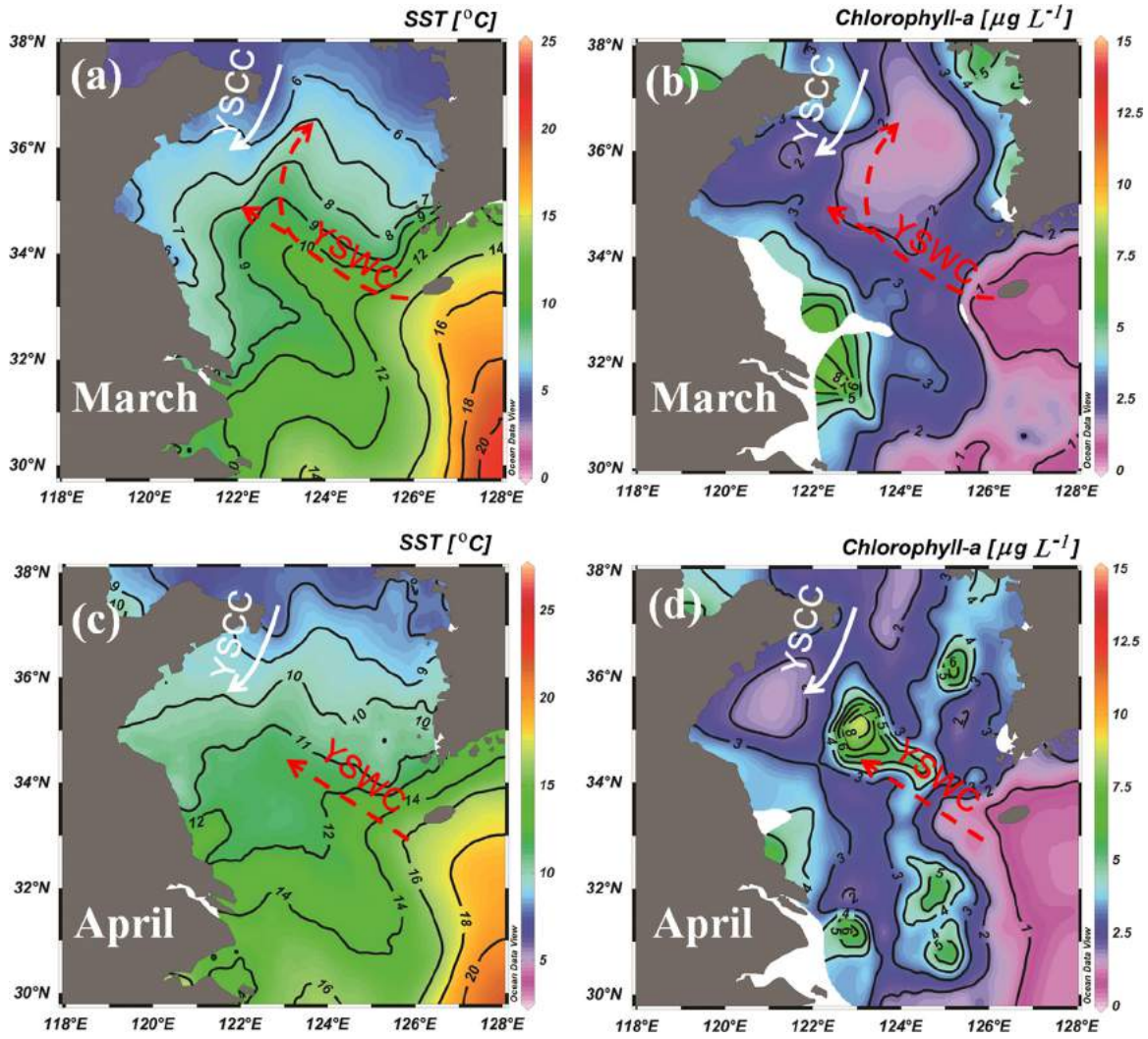

Fig. 3. Sea surface temperature (°C) and Chl *a* concentration (μg L^{-1}) based on remote sensing data during March and April 2009.
The red thick dashed lines and the white thick line indicate the axes of the warm tongues of the Yellow Sea Warm Current (YSWC) and the Yellow Sea Coastal Current (YSCC), respectively, according to Chen (2009) and Lin and Yang (2011). (For interpretation of the references to color in this figure legend, the reader is referred to the web version of this article.)

and the low density YSCC, in spite of the temperature inversion (Stn. B18, Fig. 4).

Surface nutrient concentrations increased gradually from the coastal area (the YSCC) (nitrate: ~1 μM, phosphate: 0.1 μM, silicate: 2 μM) to the central area (the YSWC) (nitrate: ~8 μM, phosphate: 0.7 μM, silicate: 12 μM) (Fig. 4). It was noted that the nutrient status contrast with the common situation of coastal waters where high salinity values usually correlate with poor nutrients. The nutrients fronts were coincident with the temperature and salinity fronts (Fig. 4). As a consequence, a good positive linear relationship was found between salinity and nitrate concentrations in the frontal area (Fig. 5, $32 < S < 33$, $p < 0.01$). The distribution of nutrient in the front water was produced by mixing between the low nutrient YSCC water and the high nutrient YSWC water (Figs. 4 and 5). Moreover, the highest nitrate concentration (> 8 μM) was observed with salinity of ~33.5, rather than the highest salinity value (Fig. 5). Both the 2007 and 2009 field observations revealed similar results (Fig. 5).

3.3. Phytoplankton biomass and community structure

Contrary to the distribution patterns of temperature and nutrients, Chl *a* concentrations were higher at the coastal stations in the YSCC water region than in the central area of the Yellow Sea (the YSWC) during March 2009 (Fig. 3b). One exception was found in the western coastal area at 36°N, which had low nutrients and Chl *a* (< 1 μg L^{-1}, Fig. 4). In the YSCC, nutrient concentrations at the low Chl *a* station (Stn. B32) seemed to be limiting (Fig. 4). On the other side, Chl *a* concentration was still low (< 1 μg L^{-1}) in the YSWC (Stn. B14) despite the fact that the nutrient concentrations and temperature were higher than those at the coastal stations (Fig. 4). The vertical distributions of biotic and abiotic environmental parameters in the YSCC and YSWC stations were homogeneous and the mixed layer depth was greater than the euphotic depth (data not shown). In contrast, weak stratification occurred in the frontal area (Stn. B18), which had high Chl *a* and low nutrient concentrations in the euphotic zone (Fig. 4). The euphotic depths in three areas, the YSCC, the YSWC and the front water, were not significantly different from each other ($p > 0.05$, $n = 11$).

The mean concentration of Fuco at the surface of the Yellow Sea was 227 ng L^{-1}, and the values were at least one magnitude higher than the other pigments. Based on CHEMTAX analysis, diatoms dominated the phytoplankton community in almost all samples, with a mean Chl *a* concentration of 583 ng L^{-1} in the surface water (Fig. 6f). In addition, the distribution pattern of diatoms was consistent with that of Chl *a* (Figs. 4f and 7f). The

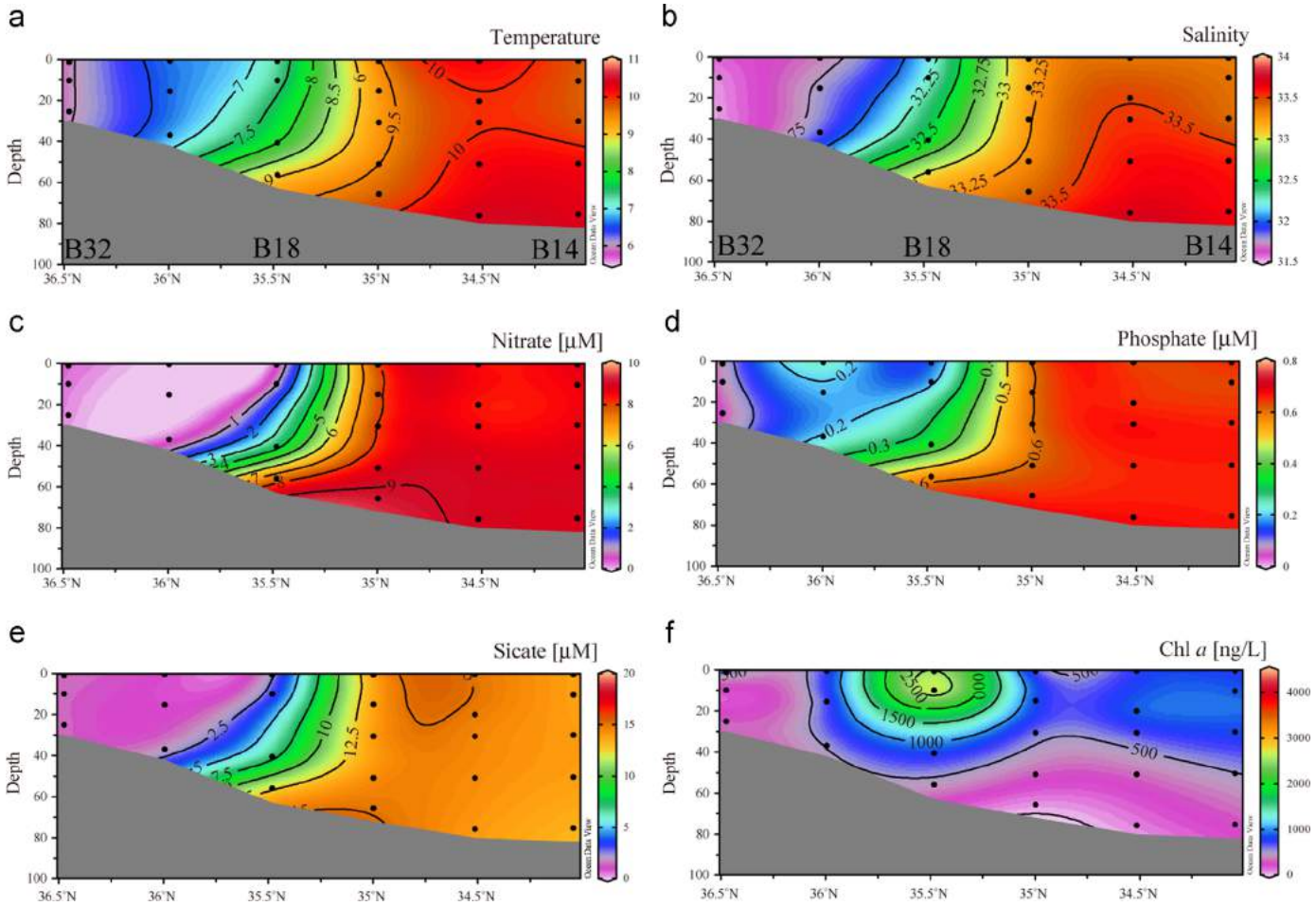

Fig. 4. Section distributions of temperature (a, °C), salinity (b), nutrients (c–e) and Chl *a* concentrations (f) from Stations B32 to B14 during March 2009.

relative abundance of diatoms compared to total Chl *a* values ranged from 26% to 90%, showing a significantly higher value in the YSCC than in YSWC waters (Fig. 8b, $p < 0.01$). Similar distributions were found between diatoms and dinoflagellates, however, the cyanobacteria and prasinophytes showed an opposite distributional pattern with the high concentration stations located in the YSWC (Figs. 6 and 7). Distributions of *Synechococcus* and eukaryotic picoplankton were similar to those of cyanobacteria and prasinophytes, respectively (Figs. 6 and 7). Their abundance in the YSWC waters were significantly higher than that in the YSCC (Fig. 8, $p < 0.05$). Similar results were observed in the 2007 cruise.

A good correlation was found between HPLC (Zea concentrations), CHEMTAX (cyanobacteria Chl *a* biomass), and flow cytometry (*Synechococcus* cell abundance) (Fig. 9). The ratios of Zea: Chl *a* and Chl *a*: cells, which are shown by the slopes in Fig. 9, were similar between the two cruises, about 0.36 and 2–3 fg cell^{-1} respectively. Similar patterns were observed in the relationships between the eukaryotic picoplankton and prasinophytes (Fig. 9).

Canonical correlation analysis was performed separately for surface and water column samples based on HPLC-CHEMTAX analyses (Fig. 10) Similar results were found between the surface and total samples. Nutrients group closely together with temperature, salinity and station depth, while Chl *a* align in the opposite direction. Diatoms are close to Chl *a*, suggesting the dominance of diatoms when Chl *a* is elevated. Cyanobacteria, *Synechococcus*, pico-eukaryotes and prasinophytes clustered apart from other groups.

Clearly, phytoplankton blooms were produced at the two time series drifter stations, with the Chl *a* concentrations in the subsurface layer over 3 and 5 μg L^{-1} (Fig. 11). During the period, the pigments concentrations at Stn. B20 were decreasing, with the total Chl *a* in the layer of subsurface Chl *a* maximum reduced by more than 80% (Fig. 11d). Diatom concentrations were at least an order of magnitude higher than those of dinoflagellates at Stn. 20. However, quite high concentrations of Peri (with the maximum of 5904 ng L^{-1}) were observed during the bloom at Stn. B23, indicating dinoflagellates dominated the community. Based on the CHEMTAX calculation, the dinoflagellate Chl *a* concentrations in the subsurface layer of Stn. B23 during 50th–80th h were over 1000 ng L^{-1}, with a mean of 444 ng L^{-1} during the study period.

4. Discussion

4.1. Nutrients sources of the YSWC

Nutrient distributions showed that nutrient-rich water invaded the central Yellow Sea along the western flank of the Yellow Sea trough, coinciding with hydrodynamic indicators of the YSWC (Fig. 4) (Jin et al., 2013; Liu et al., 2015). However, the nutrient concentrations of the YSWC were also reported to be poor in previous studies based on literature data collected in the 1970s and 1980s (Chen, 2008, 2009). Based on the time series oceanographic survey datasets measured along the coast of South Korea from the Korea Oceanography Data Center, He et al. (2013) revealed both the nitrate and phosphate concentrations increased more than two-fold between 1998 and 2005 in the southeastern

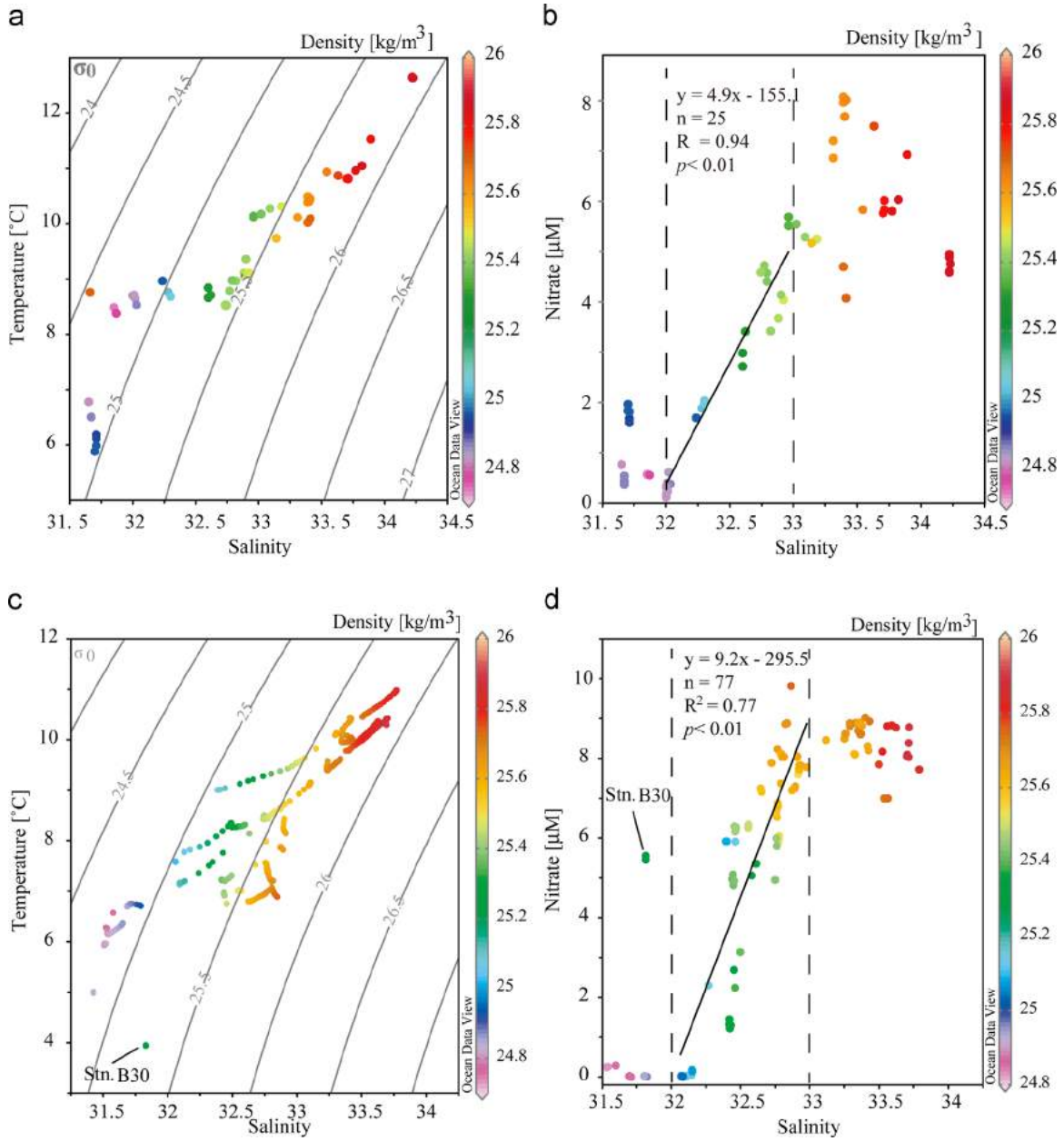

Fig. 5. The *T*/*S* diagram of all stations and the relationship between nitrate concentrations and salinity in the central Yellow Sea during March 2007 (a and b) and 2009 (c and d). Location of Stn. B30 is indicated in Fig. 1b. The density is potential density anomaly (kg m^{-3}).

Yellow Sea. In addition, the increasing trend of spring algal blooms in the central Yellow Sea (Fig. 2) was also observed from 1997–2008 (He et al., 2013; Liu and Wang, 2013; Yamaguchi et al., 2013). Therefore, it was suggested that nutrient concentrations in the YSWC have increased since the end of last century (Jin et al., 2013) and resulted in the interannual variability of Chl *a* concentrations (Fig. 2) in the central Yellow Sea (He et al., 2013).

Since the YSWC originates from the Kuroshio water and Taiwan Warm Current (Lin et al., 2011), coupled with the effects of the winter monsoon, the rich nutrient sources of the YSWC might be vertical flux from the bottom water (Jin et al., 2013), atmospheric deposition (Kim et al., 2011; Shi et al., 2013), and advective flux from the Taiwan Warm Current and the subsurface Kuroshio water (Guo et al., 2006; Liu et al., 2014). Our previous study revealed that the nutrient supply from the deep water by both diffusion and entrainment could support ca. 56% of N, 56% of P and 69% of Si for phytoplankton growth demand, and the upward nutrients fluxes from the deep water to the euphotic zone were higher than the atmospheric deposition by one to three orders of magnitude, except NH_4^+ fluxes were comparable between atmospheric input and turbulent entrainment from deep water (Jin et al., 2013).

In horizontal directions, Liu et al. (2014) reported the interannual variability of the Kuroshio onshore intrusion across the East China Sea shelf break during 1993–2010, showing a higher net Kuroshio onshore intrusion across the 200 m isobaths in years 1993, 2000–2001, 2003–2004, and 2005–2008 and lower intrusions in years 1994–1995, 1999, 2002, and 2009–2010. These are roughly in agreement with the years of increase and decease of Chl *a* concentrations in the central Yellow Sea (Fig. 2), respectively. Similar interannual variation is also found in other Kuroshio sections, indicative of the ENSO time scale of the Kuroshio variability (He and White, 1987; Akitomo et al., 1996). On the other hand, the nitrate concentration at the mouth of the Changjiang River has increased about three-fold from 1960s–2000s (Zhou et al., 2008).

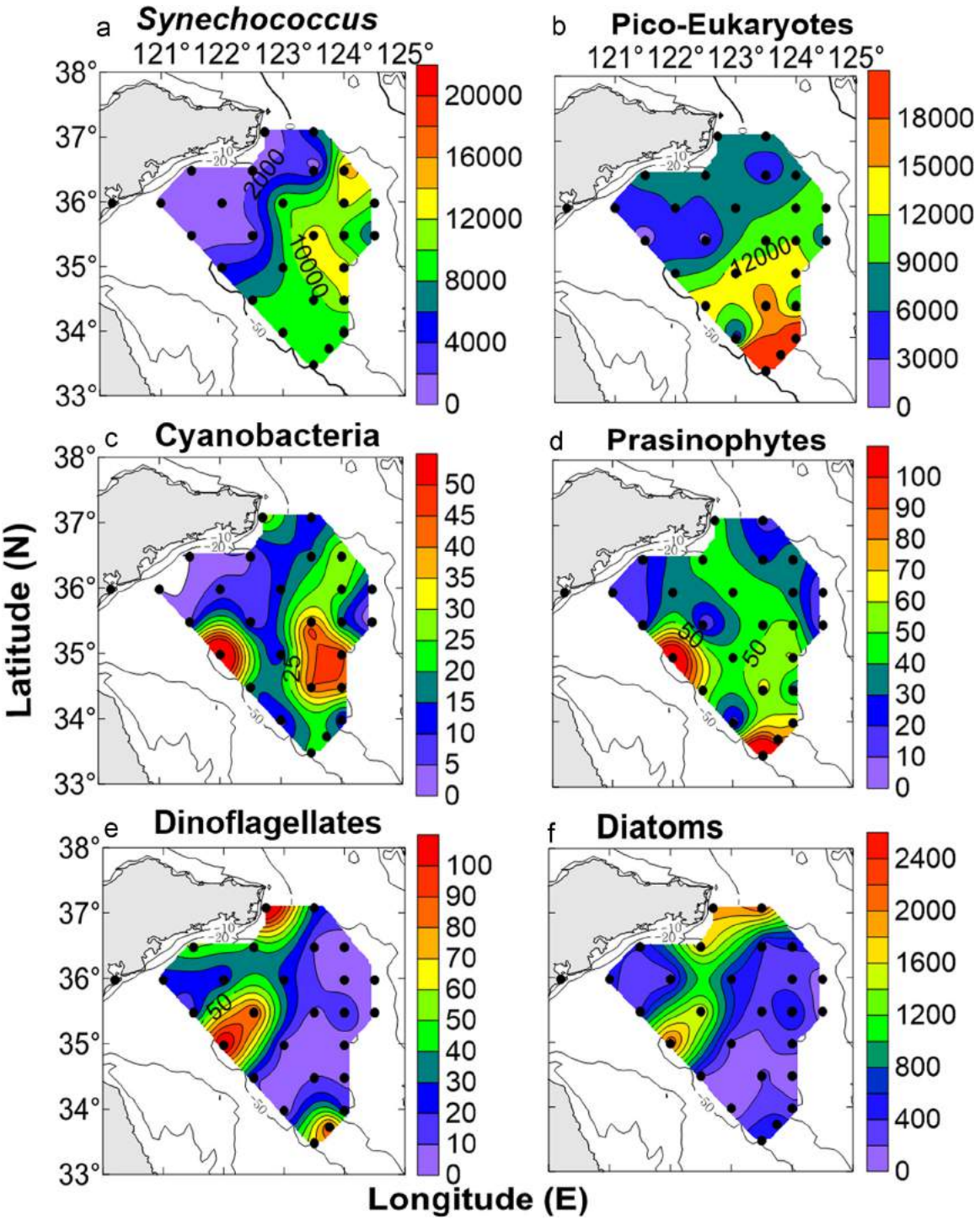

Fig. 6. Surface abundances of *Synechococcus* (cells mL^{-1}), pico-eukaryotes (cells mL^{-1}) based on flow cytometry analysis and Chl *a* concentrations (ng L^{-1}) of cyanobacteria, prasinophytes, dinoflagellates and diatoms based on HPLC-CHEMTAX analysis during March 2009.

Therefore, it is possible that the interannual variability of nutrient and Chl *a* concentrations in the central Yellow Sea are related to the changing phase in the ENSO and/or increased nutrient loading from anthropogenic activities in China. To solve this question, it is important to judge whether rich nutrients came from the original YSWC or whether the local nutrient-rich waters when the YSWC invaded the Yellow Sea from the north of the Changjiang estuary.

Our results show the positive correlation existed only in the front, and the highest nitrate concentrations (>8 μM) were observed not in the water with the highest salinity (Fig. 5b). We summarized the temperature, salinity and nutrient concentrations of the YSWC and the potential sources according to Chen (2009) (Table 1). The nitrate concentration in the original water from bottom of the Jeju Warm Current are about 3–5 μM with salinity of 33.5–34.5, which match our results at the salinity of 34 (Fig. 5b). On the other hand, nitrate in the bottom water above the Changjiang Bank (the East China Sea Dense Water) are much higher (5–14 μM) with lower salinity values (32–34, Table 1). The averaged nutrients concentrations in the YSWC are higher than those of the Jeju Warm Current (Table 1). Based on mooring observations, a strong vertical shear velocity at the westward YSWC was observed when it invaded the Yellow Sea from the north of the Changjiang estuary; the surface current was westward

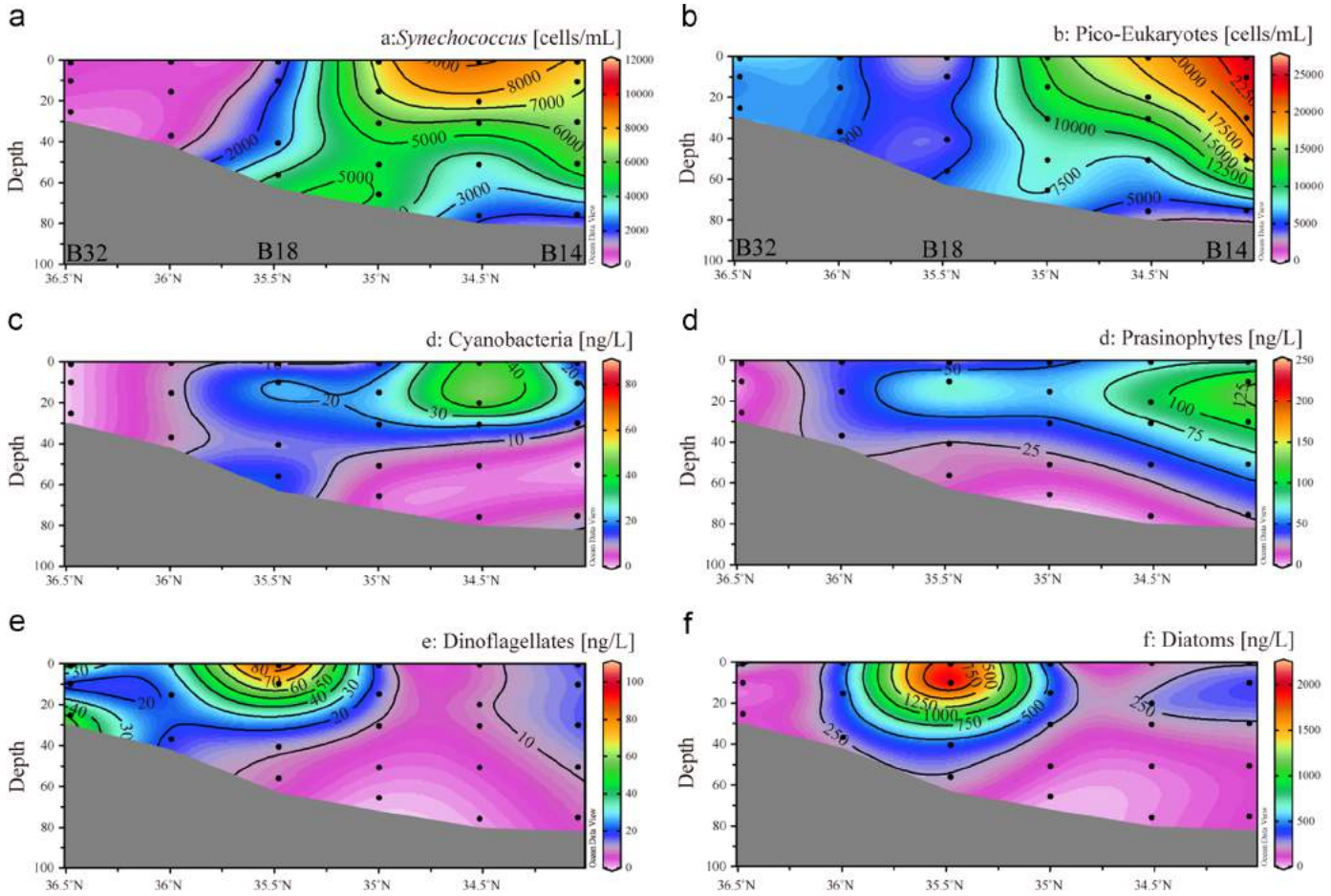

Fig. 7. Section distributions of *Synechococcus* (cells mL^{-1}), pico-eukaryotes (cells mL^{-1}) based on flow cytometry analysis and Chl *a* concentrations (ng L^{-1}) of cyanobacteria, prasinophytes, dinoflagellates and diatoms based on HPLC analysis from Stations B32 to B14 March 2009.

while the water in the subsurface layer was northward (Lin and Yang, 2011). This northward subsurface current is associated with the Ekman and baroclinic current (Lin and Yang, 2011), which may transport the water of the Changjiang Bank to the Yellow Sea trough. Therefore, nutrient concentrations of the YSWC waters might have been enhanced by this process, explaining for the decline in nutrients when the salinity was higher (Fig. 5). Further study, especially more field results close to the shelf break where the Kuroshio branch impinges upon the Yellow Sea and model analysis should pay attention to the nutrient contributions of these sources to the YSWC.

4.2. Phytoplankton in the YSCC and YSWC

In the coastal area, nutrient concentrations are expected to be high and, thus, the phytoplankton growth is considered to be limited by light availability (Liu et al., 2015). However, it is noted that the nutrient and Chl *a* concentrations in some parts of the western coastal area are lower than in the other YSCC areas (Figs. 3 and 4). During early spring, such low nutrient concentrations are observed occasionally in coastal areas (Chen, 2009; Fu et al., 2009). Comparison of the hydrologic and chemical environment between stations in the YSCC indicated that nutrient concentrations at the low Chl *a* station (Stn. B32) were lower than those at the high Chl *a* station (Stn. B30), while similar depths of the euphotic zone were observed between them. These results imply that phytoplankton growth in the coastal water could also be limited by nutrients not only light.

Our results reveal that diatoms dominated the phytoplankton community in almost all samples, especially in the YSCC and front water (Figs. 6f and 7f). Microscopical analyses on the same cruises revealed that the diatoms *Paralia sulcata* and *Coscinodiscus* spp. dominated the phytoplankton community in the coastal area, contributing 22% and 28% of the total Utermöhl phytoplankton abundance (Utermöhl, 1958; Tian, 2011). Diatoms generally thrive in turbulent coastal environments where strong tidal and wind mixing prevail (Reynolds, 2006; Liu et al., 2015). Small diatoms typically exhibit a "velocity" strategy, with high maximum rates of nutrient uptake and growth, while large diatoms tend to be more "storage adapted", with disproportionately large storage vacuoles (Sommer, 1984; Litchman et al., 2007). Thus, diatoms, as a group, have varying advantages that contribute to their relative success under conditions of both high and fluctuating nutrients.

Our results indicate that the abundance of cyanobacteria and eukaryotic picoplankton groups were significantly higher in the YSWC than in the YSCC waters based both on pigment and flow cytometry results (Figs. 6–8). Liu et al. (2015) noted that prasinophytes are more abundant in the central area in winter, and that is further supported by the present data (Fig. 7d). It is clear that the biota are different on either side of the front (Fig. 7). Diatoms and picophytoplankton are usually observed abundant in the cold coastal water and the warm Kuroshio water, respectively (Furuya et al., 2003), however, in the nutrient-rich water low relative abundance of diatoms with abundant picophytoplankton are unusual (Fig. 8b).

In the YSWC, where nutrient and temperature were high, the most likely limiting factor of phytoplankton growth is the light availability as a result of strong vertical mixing. Our results show the ratios of Zea to Chl *a* (0.36, Fig. 9) were very close to the values

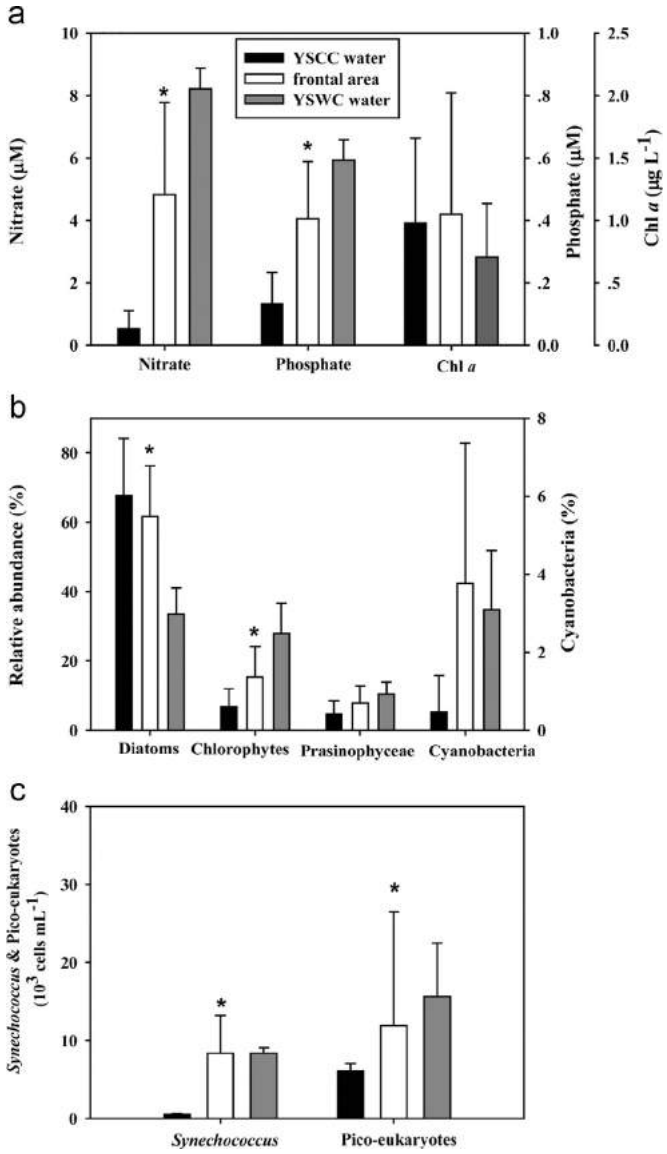

Fig. 8. Comparisons between different water masses on the concentrations of nutrients and Chl *a* (a), Chl *a* biomass of the major phytoplankton groups (b), and abundance of *Synechococcus* and pico-eukaryotes (c) based on CHEMTAX or flow cytometry analysis in the surface water of the Yellow Sea during March 2009. Results of Stn. B30 are not included in the YSCC water. Asterisk in the histograms indicate there is a significant difference within groups by one-way ANOVA.

of low light types in culture and in the field (Higgins et al., 2011), indicating insufficient light in the YSWC. Indeed, previous studies revealed that stability of the water column is a key factor for the increase of phytoplankton biomass in the central Yellow Sea during the early spring (Zhou et al., 2013; Liu et al., 2015). In fact, compared to the other groups photo adaptation capability of diatoms allows them to tolerate high and low light intensities corresponding to different depths of the mixed layer (Simpson and Sharples, 2012). If diatoms in the YSWC and the YSCC are similar species, they should be more advantageous in the nutrient-rich YSWC water. Furthermore, sectional distributional patterns of the picophytoplankton were consistent with those of temperature and salinity, and their abundances suddenly decreased at the front (Fig. 7). Therefore, it seems that the front separates the YSWC from the coastal water, and different phytoplankton groups are transported in these water masses and follow their movement (Figs. 6–8).

A good correlation between cyanobacteria Chl *a* biomass and Zea (Fig. 9) was observed. Because of the absence of *Prochlorococcus* in the Yellow Sea (Liu et al., 2015), the specificity of Zea in the cyanobacteria is much higher than when *Prochlorococcus* and *Synechococcus* coexist (Higgins et al., 2011), and strong vertical mixing reduces the effects of light on the ratio between Zea and Chl *a* at different depths (Furuya et al., 2003). For these reasons the accuracy of the CHEMTAX calculation was improved, and thus the data from HPLC and flow cytometry were consistent. In the case of the pico-eukaryotes, the composition is complex. Chrysophytes, prymnesiophytes, chlorophytes and prasinophytes are all considered as important contributors. Our results suggest that prasinophytes might be the major group of pico-eukaryotes in the central Yellow Sea during the study period as similar distributional patterns (Figs. 6 and 7) and significant correlations between them (Figs. 9 and 10).

These small-sized photosynthetic members of the eukaryotic phytoplankton are identified in several studies as mixotrophic and major predators of prokaryotes (Zubkov and Tarran, 2008; McKie-Krisberg and Sanders, 2014). Mixotrophy, the combination of photosynthesis and phagotrophy in a single organism, is well established for most photosynthetic lineages (McKie-Krisberg and Sanders, 2014) and plays an important role in marine ecosystems (Mitra et al., 2014). Although they are ubiquitous and very important in biogeochemical cycles, few studies have been reported on these groups in the Yellow Sea. Future studies should investigate the distribution and dynamics in these groups since they make up a large part of the small-sized eukaryotic phytoplankton, influencing both biomass and primary production in the YSWC.

During the early spring, due to the strengthened stratification, residence time of phytoplankton in the euphotic zone increased and the vertical supply of nutrients gradually decreased (Jin et al., 2013; Zhou et al., 2013). Consequently, Chl *a* concentration increased as nutrient concentrations decreased (Jin et al., 2013; Zhao et al., 2013). However, the intensifications of stratification during the blooms at the two time series stations were different (Zhou et al., 2013). The water column at Stn. B23 was gradually stratified as a result of increasing surface temperature, while the stratification at Stn. B20 (frontal area) was mainly driven by the salinity variations (Zhou et al., 2013). More importantly, the pigments results suggested different dominated groups at bloom stations B20 and B23 (Fig. 11). Combined with microscopical analyses, *Heterocapsa lanceolata* and *Prorocentrum minimum* were confirmed as the main phytoplankton species (dinoflagellates) during bloom Stn. B23 (Tang et al., 2013; Zhao et al., 2013). While, at Stn. B20 the dominant species were replaced by diatoms (*Detonula pumila* and *Guinardia delicatula*). As the temperature differed between these two stations, this can be possibly be explained by the species-specific effects of temperature on many aspects of dinoflagellates physiology. By contrast, diatom blooms are presumably dependent on day length or light intensity rather than on temperature-mediated physiological responses in their life strategies (Edwards and Richardson, 2004). Nevertheless, the blooms dominated by different phytoplankton (Fig. 11) were triggered by two different mechanisms in the central Yellow Sea during April 2009. One was associated with the northwestward intrusion of the YSWC, while the other was more closely linked to increasing surface temperature (Zhou et al., 2013).

5. Conclusions

The present study shows phytoplankton communities are different on either side of the front between the warm saline YSWC and the cold fresh YSCC. The oceanic YSWC water does have a nutrient-rich characteristic. Nutrient concentrations of the YSWC waters might have been enhanced by mixing with the local

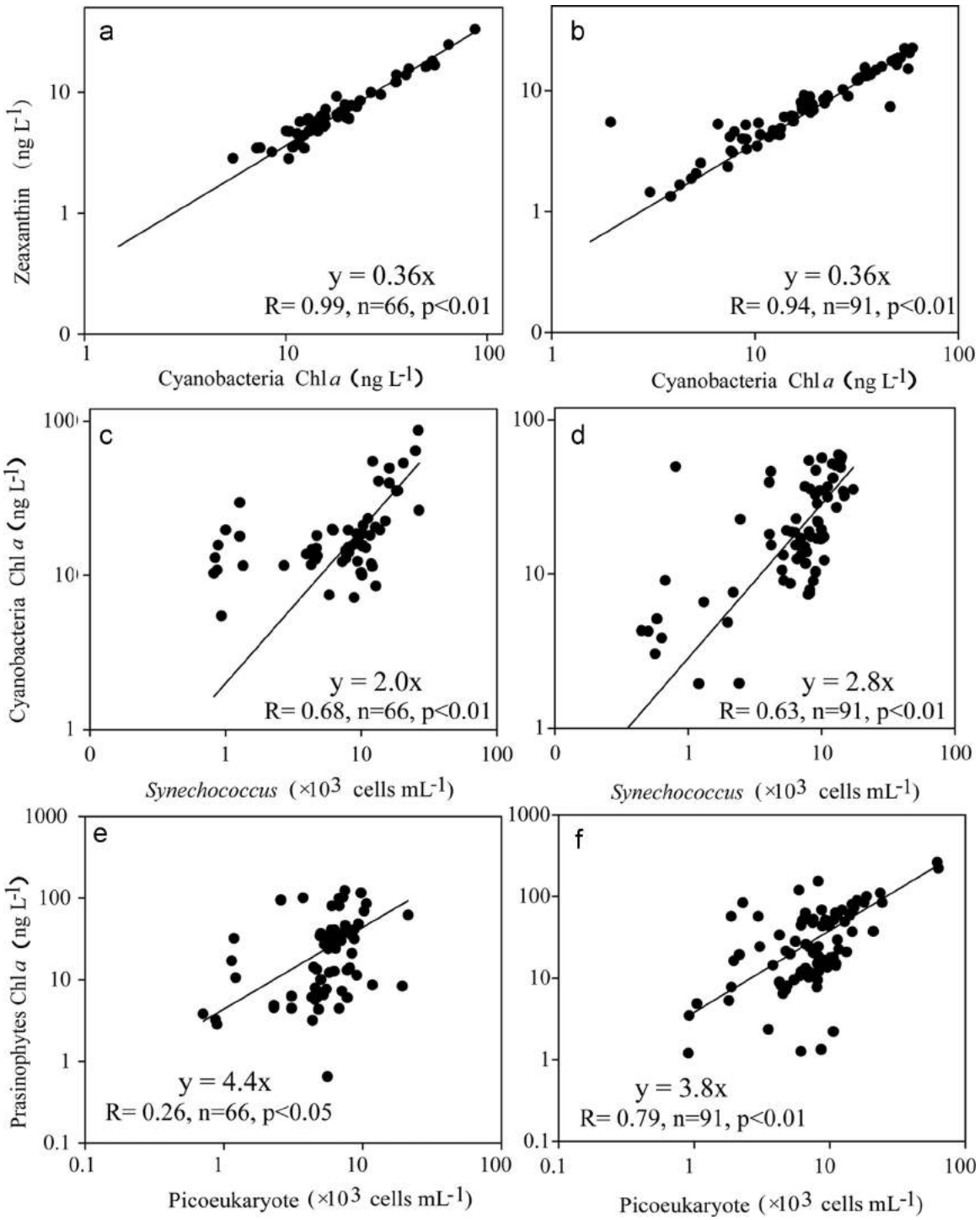

Fig. 9. Comparison of the results between HPLC, CHEMTAX and flow cytometry analyses during March 2007 (a, c and e) and 2009 (b, d and f). These results are concentrations of zeaxanthin and Chl *a* biomass of cyanobacteria using HPLC and CHEMTAX analyses, respectively (a and d); Chl *a* biomass of cyanobacteria and abundance of *Synechococcus* using CHEMTAX and flow cytometry analyses, respectively (c and d); Chl *a* concentrations of prasinophytes and abundance of pico-eukaryotes using CHEMTAX and flow cytometry analyses, respectively (e and f).

nutrient-rich waters when it invaded the Yellow Sea from the north of the Changjiang estuary. Diatoms and dinoflagellates are abundant in the YSCC, however the cyanobacteria and prasinophytes show an opposite distributional pattern. Consistent results are obtained based on the pigments and flow cytometry measurements. Our results suggest that prasinophytes might be the major group of pico-eukaryotes in the central Yellow Sea. Further study on these small-sized eukaryotic phytoplankton is suggested. It seems that different phytoplankton groups separated by the front are transported in the water masses, and followed their movement. All these results indicate the YSWC plays important roles in the distribution of nutrients, phytoplankton biomass and also community structure in the central Yellow Sea. This study highlights the complexity of ecosystem in coastal areas.

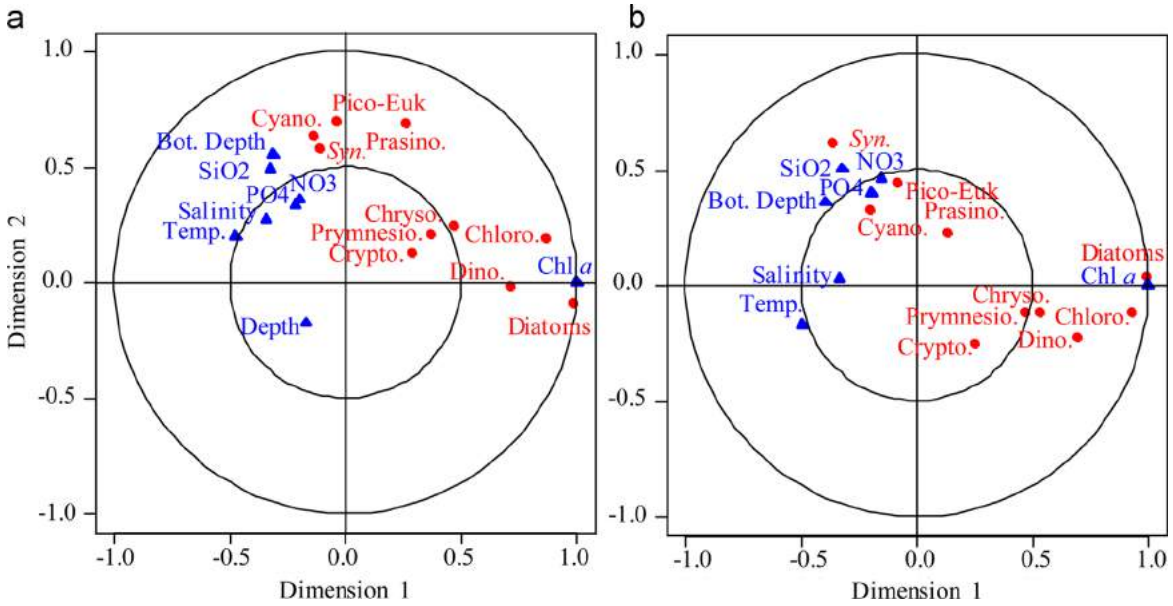

Fig. 10. Canonical correspondence analysis plot using abundance of *Synechococcus* and pico-eukaryotes (Pico-Euk), Chl *a* concentrations of 8 different phytoplankton groups (HPLC-CHEMTAX) and environmental parameters (temperature, salinity, concentrations of nitrate, phosphate and silicate, bottom depth and sample depth for surface (a, $n=25$) and water column samples (b, $n=86$)) during March 2009.

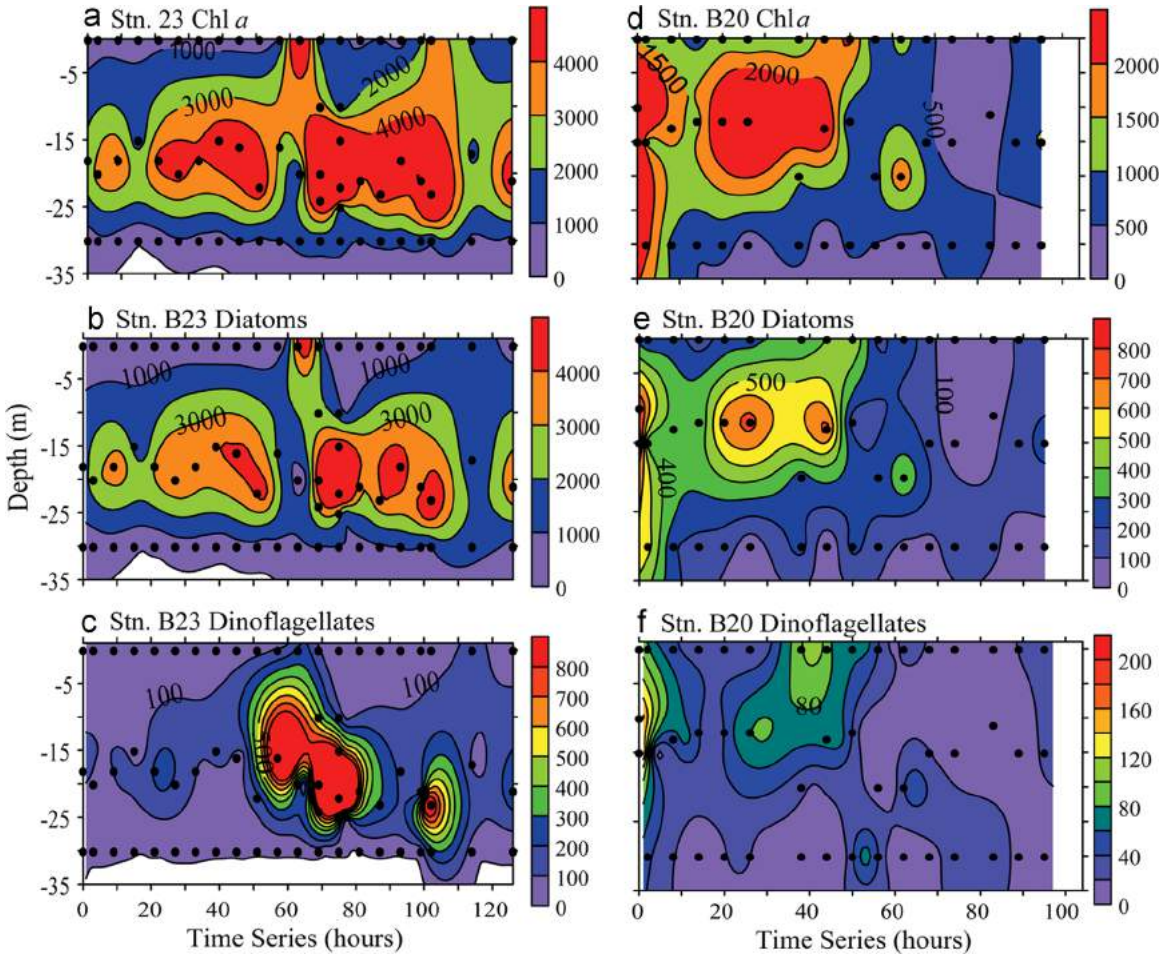

Fig. 11. Time series observations on concentrations (ng L^{-1}) of Chl *a*, diatoms and dinoflagellates in the up 35 m at Stns. B20 and B23 (Fig. 1b) during time series observations in March 2009.

Table 1
Summarized the temperature, salinity and nutrients concentrations at the surface and bottom water of the YSWC and the potential sources, the Jeju Warm Current (JWC) and the East China Sea Dense Water (ECSDW) during winter.

	T (°C)	S	NO_3 (μM)	PO_4 (μM)	SiO_2 (μM)	References
Surface						
YSCC	6.0 ± 0.7	31.6 ± 0.1	0.5 ± 0.6	0.1 ± 0.1	1.3 ± 0.2	This study
YSWC	9.76 ± 0.7	33.3 ± 0.4	7.9 ± 1.0	0.6 ± 0.1	13.1 ± 1.2	This study
JWC	10–15	33.5–34.5	1–3	0.2–0.4	<5–10	Chen (2009)
ECSDW	9–13	32–34	5–12	0.4–0.6	5–20	Chen (2009)
Bottom						
YSCC	5.6 ± 1.1	31.7 ± 0.2	1.2 ± 2.5	0.2 ± 0.2	2.0 ± 1.3	This study
YSWC	10.0 ± 0.9	33.5 ± 0.3	8.5 ± 0.5	0.6 ± 0.1	13.0 ± 1.0	This study
JWC	10–13	33.5–34.5	3–5	0.2–0.4	5–10	Chen (2009)
ECSDW	9–15	32–34	5–14	0.4–0.8	5–15	Chen (2009)

Acknowledgments

This work was supported by Grants from the National Basic Research Programme (No. 2011CB403603), the China NSF (Nos. U1406403, 41176112 and 41406143) and Chinese Academy of Science project (XDA11020103). All data of the present study can be found in the China GLOBEC-IMBER committee website (www.globec-imber.ac.cn). We thank Prof. Jun Sun of the Tianjin University of Science and Technology for phytoplankton identification. We thank Prof. John Hodgkiss of The University of Hong Kong and Prof. Michael R. Landry of Scripps Institution of Oceanography for their English language editing and comments on the manuscript. The authors would like to thank the captain and crew of the R/V "Beidou", who made concerted efforts to assist during field sampling. We also show our thanks to the anonymous reviewers.

References

Akitomo, K., Ooi, M., Awaji, T., Kutsuwada, K., 1996. Interannual variability of the Kuroshio transport in response to the wind stress field over the north Pacific: its relation to the path variation south of Japan. J. Geophys. Res.-Oceans 101, 14057–14071. http://dx.doi.org/10.1029/96jc01000.

Behrenfeld, M.J., Boss, E.S., 2014. Resurrecting the ecological underpinnings of ocean plankton blooms. Annu. Rev. Mar. Sci. 6, 167–194. http://dx.doi.org/10.1146/annurev-marine-052913-021325.

Chen, C.T.A., 2008. Distributions of nutrients in the East China Sea and the South China Sea connection. J. Oceanogr. 64, 737–751. http://dx.doi.org/10.1007/s10872-008-0062-9.

Chen, C.T.A., 2009. Chemical and physical fronts in the Bohai, Yellow and East China seas. J. Mar. Syst. 78, 394–410. http://dx.doi.org/10.1016/j.jmarsys.2008.11.016.

Du, C., Liu, Z., Dai, M., Kao, S.J., Cao, Z., Zhang, Y., Huang, T., Wang, L., Li, Y., 2013. Impact of the Kuroshio intrusion on the nutrient inventory in the upper northern South China Sea: insights from an isopycnal mixing model. Biogeosciences 10, 6419–6432. http://dx.doi.org/10.5194/bg-10-6419-2013.

Edwards, M., Richardson, A.J., 2004. Impact of climate change on marine pelagic phenology and trophic mismatch. Nature 430, 881–884. http://dx.doi.org/10.1038/nature02808.

Fu, M.Z., Wang, Z.L., Li, Y., Li, R.X., Sun, P., Wei, X.H., Lin, X.Z., Guo, J.S., 2009. Phytoplankton biomass size structure and its regulation in the Southern Yellow Sea (China): seasonal variability. Cont. Shelf Res. 29, 2178–2194. http://dx.doi.org/10.1016/j.csr.2009.08.010.

Furuya, K., Hayashi, M., Yabushita, Y., Ishikawa, A., 2003. Phytoplankton dynamics in the East China Sea in spring and summer as revealed by HPLC-derived pigment signatures. Deep Sea Res. Part II: Top. Stud. Oceanogr. 50, 367–387. http://dx.doi.org/10.1016/S0967-0645(02)00460-5.

González, I., Déjean, S., Martin, P.G., Baccini, A., 2008. CCA: an R package to extend canonical correlation analysis. J. Stat. Softw. 23, 1–14.

Guo, X., Miyazawa, Y., Yamagata, T., 2006. The Kuroshio onshore intrusion along the shelf break of the East China Sea: the origin of the Tsushima Warm Current. J. Phys. Oceanogr. 36, 2205–2231. http://dx.doi.org/10.1175/Jpo2976.1.

He, X., Bai, Y., Pan, D., Chen, C.T.A., Cheng, Q., Wang, D., Gong, F., 2013. Satellite views of the seasonal and interannual variability of phytoplankton blooms in the eastern China seas over the past 14 yr (1998–2011). Biogeosciences 10, 4721–4739. http://dx.doi.org/10.5194/bg-10-4721-2013.

He, Y.H., White, W.B., 1987. Interannual variability of the Kuroshio frontal structure along its western boundary in the North Pacific-Ocean associated with the 1982-Enso event. J. Phys. Oceanogr. 17, 1494–1506. http://dx.doi.org/10.1175/1520-0485(1987).

Higgins, H.W., Wright, S.W., Schlüter, L., 2011. Quantitative interpretation of chemotaxonomic pigment data. In: Roy, S., Llewellyn, C.A., Egeland, E.S., Johnsen, G. (Eds.), Phytoplankton Pigments. Cambridge University Press, United Kingdom.

Hu, D.X., Wu, L.X., Cai, W.J., Sen Gupta, A., Ganachaud, A., Qiu, B., Gordon, A.L., Lin, X. P., Chen, Z.H., Hu, S.J., Wang, G.J., Wang, Q.Y., Sprintall, J., Qu, T.D., Kashino, Y., Wang, F., Kessler, W.S., 2015. Pacific western boundary currents and their roles in climate. Nature 522, 299–308. http://dx.doi.org/10.1038/nature14504.

Hu, H.G., Wan, Z.W., Yuan, Y.L., 2004. Simulation of seasonal variation of phytoplankton in the southern Huanghai (Yellow) Sea and analysis on its influential factors. Acta Oceanol. Sin. 26, 74–88.

Huang, D., Fan, X., Xu, D., Tong, Y., Su, J., 2005. Westward shift of the Yellow Sea warm salty tongue. Geophys. Res. Lett. 32, L24613, http://dx.doi.org/10.1029/2005GL024749.

Hyun, J.H., Kim, K.H., 2003. Bacterial abundance and production during the unique spring phytoplankton bloom in the central Yellow Sea. Mar. Ecol. Prog. Ser. 252, 77–88. http://dx.doi.org/10.3354/Meps252077.

Jin, J., Liu, S.M., Ren, J.L., Liu, C.G., Zhang, J., Zhang, G.L., Huang, D.J., 2013. Nutrient dynamics and coupling with phytoplankton species composition during the spring blooms in the Yellow Sea. Deep Sea Res. Part II: Top. Stud. Oceanogr. 97, 16–32. http://dx.doi.org/10.1016/j.dsr2.2013.05.002.

Kim, T.W., Lee, K., Najjar, R.G., Jeong, H.D., Jeong, H.J., 2011. Increasing N abundance in the northwestern Pacific Ocean due to atmospheric nitrogen deposition. Science 334, 505–509. http://dx.doi.org/10.1126/science.1206583.

Latasa, M., 2007. Improving estimations of phytoplankton class abundances using CHEMTAX. Mar. Ecol. Prog. Ser. 329, 13–21. http://dx.doi.org/10.3354/Meps329013.

Lie, H.J., Cho, C.H., Lee, J.H., Lee, S., Tang, Y.X., Zou, E.M., 2001. Does the Yellow Sea Warm Current really exist as a persistent mean flow? J. Geophys. Res.-Oceans 106, 22199–22210. http://dx.doi.org/10.1029/2000jc000629.

Lie, H.J., Cho, C.H., Lee, S., 2009. Tongue-shaped frontal structure and warm water intrusion in the southern Yellow Sea in winter. J. Geophys. Res.-Oceans 114, C01003. http://dx.doi.org/10.1029/2007JC004683.

Lin, X.P., Yang, J.Y., 2011. An asymmetric upwind flow, Yellow Sea Warm Current: 2. Arrested topographic waves in response to the northwesterly wind. J. Geophys. Res.-Oceans 116, C04027. http://dx.doi.org/10.1029/2010jc006514.

Lin, X.P., Yang, J.Y., Guo, J.S., Zhang, Z.X., Yin, Y.Q., Song, X.Z., Zhang, X.H., 2011. An asymmetric upwind flow, Yellow Sea Warm Current: 1. New observations in the western Yellow Sea. J. Geophys. Res.-Oceans 116, C04026. http://dx.doi.org/10.1029/2010jc006513.

Litchman, E., Klausmeier, C.A., Schofield, O.M., Falkowski, P.G., 2007. The role of functional traits and trade-offs in structuring phytoplankton communities: scaling from cellular to ecosystem level. Ecol. Lett. 10, 1170–1181. http://dx.doi.org/10.1111/j.1461-0248.2007.01117.x.

Liu, C.Y., Wang, F., Chen, X.P., von Storch, J.S., 2014. Interannual variability of the Kuroshio onshore intrusion along the East China Sea shelf break: effect of the Kuroshio volume transport. J. Geophys. Res.-Oceans 119, 6190–6209. http://dx.doi.org/10.1002/2013jc009653.

Liu, D., Wang, Y., 2013. Trends of satellite derived chlorophyll-a (1997–2011) in the Bohai and Yellow Seas, China: effects of bathymetry on seasonal and interannual patterns. Prog. Oceanogr. 116, 154–166. http://dx.doi.org/10.1016/j.pocean.2013.07.003.

Liu, X., Huang, B.Q., Huang, Q., Wang, L., Ni, X.B., Tang, Q.S., Sun, S., Wei, H., Liu, S.M., Li, C.L., Sun, J., 2015. Seasonal phytoplankton response to physical processes in the southern Yellow Sea. J. Sea Res. 95, 45–55. http://dx.doi.org/10.1016/j.seares.2014.10.017.

Liu, X., Huang, B.Q., Liu, Z.Y., Wang, L., Wei, H., Li, C.L., Huang, Q., 2012. High-resolution phytoplankton diel variations in the summer stratified central Yellow Sea. J. Oceanogr. 68, 913–927. http://dx.doi.org/10.1007/s10872-012-0144-6.

Mackey, M.D., Mackey, D.J., Higgins, H.W., Wright, S.W., 1996. CHEMTAX – a program for estimating class abundances from chemical markers: application to HPLC measurements of phytoplankton. Mar. Ecol. Prog. Ser. 144, 265–283. http://dx.doi.org/10.3354/Meps144265.

Marie, D., Simon, N., Guillou, L., Partensky, F., Vaulot, D., 2000. Flow cytometry analysis of marine picoplankton In Living Color. Springer, pp. 421–454.

McKie-Krisberg, Z.M., Sanders, R.W., 2014. Phagotrophy by the picoeukaryotic green alga micromonas: implications for Arctic Oceans. ISME J. 8, 1953–1961. http://dx.doi.org/10.1038/ismej.2014.16.

Mitra, A., Flynn, K.J., Burkholder, J.M., Berge, T., Calbet, A., Raven, J.A., Granéli, E., Glibert, P.M., Hansen, P.J., Stoecker, D.K., Thingstad, F., Tillmann, U., Våge, S., Wilken, S., Zubkov, M.V., 2014. The role of mixotrophic protists in the biological carbon pump. Biogeosciences 11, 995–1005. http://dx.doi.org/10.5194/bg-11-995-2014.

Olson, R.J., Zettler, E.R., DuRand, M.D., 1993. Phytoplankton analysis using flow cytometry, Handbook of methods in Aquat. Microb. Ecol., pp. 175–186.

Reynolds, C.S., 2006. Ecology of Phytoplankton. Cambridge University Press, New York.

Shi, J.-H., Zhang, J., Gao, H.-W., Tan, S.-C., Yao, X.-H., Ren, J.-L., 2013. Concentration, solubility and deposition flux of atmospheric particulate nutrients over the Yellow Sea. Deep Sea Res. Part II: Top. Stud. Oceanogr. 97, 43–50. http://dx.doi.

org/10.1016/j.dsr2.2013.05.004.
Simpson, J.H., Sharples, J., 2012. Introduction to the Physical and Biological Oceanography of Shelf Seas. Cambridge University Press, United Kingdom.
Sommer, U., 1984. The paradox of the plankton: fluctuations of phosphorus availability maintain diversity of phytoplankton in flow-through cultures. Limnol. Oceanogr. 29, 633–636.
Sun, J., Feng, Y., Zhou, F., Song, S., Jiang, Y., Ding, C., 2013. Top-down control of spring surface phytoplankton blooms by microzooplankton in the Central Yellow Sea, China. Deep Sea Res. Part II: Top. Stud. Oceanogr. 97, 51–60. http://dx.doi.org/10.1016/j.dsr2.2013.05.005.
Tang, Q., Su, J., Zhang, J., Tong, L., 2013. Spring blooms and the ecosystem processes: the case study of the Yellow Sea. Deep Sea Res. Part II: Top. Stud. Oceanogr. 97, 1–3. http://dx.doi.org/10.1016/j.dsr2.2013.05.007.
Tian, W., 2011. Phytoplankton community structure and species succession in bloom of central Yellow Sea 2009 (Master Thesis). Ocean University of China Qingdao, China.
Utermöhl, H., 1958. Zur vervollkommnung der quantitativen phytoplankton-methodik. Mitt. Int. Ver. Theor. unde Amgewandte Limnol. 9, 1–38.
Wang, F., Liu, C., Meng, Q., 2012. Effect of the Yellow Sea warm current fronts on the westward shift of the Yellow Sea warm tongue in winter. Cont. Shelf Res. 45, 98–107. http://dx.doi.org/10.1016/j.csr.2012.06.005.
Xuan, J.-L., Zhou, F., Huang, D.-J., Wei, H., Liu, C.-G., Xing, C.-X., 2011. Physical processes and their role on the spatial and temporal variability of the spring phytoplankton bloom in the central Yellow Sea. Acta Ecol. Sin. 31, 61–70. http://dx.doi.org/10.1016/j.chnaes.2010.11.011.
Yamaguchi, H., Ishizaka, J., Siswanto, E., Son, Y.B., Yoo, S., Kiyomoto, Y., 2013. Seasonal and spring interannual variations in satellite-observed chlorophyll-a in the Yellow and East China Seas: new datasets with reduced interference from high concentration of resuspended sediment. Cont. Shelf Res. 59, 1–9. http://dx.doi.org/10.1016/j.csr.2013.03.009.
Yang, D., Yin, B., Liu, Z., Bai, T., Qi, J., Chen, H., 2012. Numerical study on the pattern and origins of Kuroshio branches in the bottom water of southern East China Sea in summer. J. Geophys. Res. 117, C02014. http://dx.doi.org/10.1029/2011jc007528.
Zapata, M., Rodriguez, F., Garrido, J.L., 2000. Separation of chlorophylls and carotenoids from marine phytoplankton: a new HPLC method using a reversed phase C_8 column and pyridine-containing mobile phases. Mar. Ecol. Prog. Ser. 195, 29–45. http://dx.doi.org/10.3354/Meps195029.
Zhao, Y., Zhao, L., Xiao, T., Liu, C., Sun, J., Zhou, F., Liu, S., Huang, L., 2013. Temporal variation of picoplankton in the spring bloom of Yellow Sea, China. Deep Sea Res. Part II: Top. Stud. Oceanogr. 97, 72–84. http://dx.doi.org/10.1016/j.dsr2.2013.05.015.
Zhou, F., Xuan, J., Huang, D., Liu, C., Sun, J., 2013. The timing and the magnitude of spring phytoplankton blooms and their relationship with physical forcing in the central Yellow Sea in 2009. Deep Sea Res. Part II: Top. Stud. Oceanogr. 97, 4–15. http://dx.doi.org/10.1016/j.dsr2.2013.05.001.
Zhou, M.J., Shen, Z.L., Yu, R.C., 2008. Responses of a coastal phytoplankton community to increased nutrient input from the Changjiang (Yangtze) River. Cont. Shelf Res. 28, 1483–1489. http://dx.doi.org/10.1016/j.csr.2007.02.009.
Zubkov, M.V., Tarran, G.A., 2008. High bacterivory by the smallest phytoplankton in the North Atlantic Ocean. Nature 455, 224–226. http://dx.doi.org/10.1038/nature07236.